1.B

Nuclear Physics A278 (1977) 491–505;

MULTIPLE PION EXCHANGE IN A NONSTATIC THEORY OF NUCLEON-NUCLEON SCATTERING AND ISOBAR PRODUCTION

H. J. WEBER [†]

Department of Physics, University of Virginia, Charlottesville, Virginia 22901, USA

and

J. M. EISENBERG [††] and M. D. SHUSTER [†††]

Department of Physics and Astronomy, Tel-Aviv University, Ramat-Aviv, Tel-Aviv, Israel

Received 16 August 1976

(Revised 1 November 1976)

Abstract: Exchange of nonstatic pions between a nucleon and Δ(1231) isobar in the reactions NN → NN and NN → NΔ is studied near the pion- and Δ-production thresholds. The nonstatic nature of the exchange permits the repeated formation and decay of a nearly on-shell isobar as the pion shuttles back and forth on its mass shell. The mechanism modifies the analysis of NN elastic and Δ production processes at intermediate range ($\approx \frac{1}{2}M_\pi^{-1}$). We examine these effects in a relativistic theory, restricted to spinless particles, based on the covariant off-shell formalism of Blankenbecler and Sugar. Three versions of this theory are considered, involving intermediate nucleon-isobar propagation taken off the mass shell (i) symmetrically, (ii) nonsymmetrically, and (iii) in a quasiparticle formulation. For the mechanism considered here, a clear preference is found for the nonsymmetrical prescription. Our results indicate that the nonstatic multiple-pion-exchange mechanism should be included in quantitative analyses of NN → NN, NΔ in the threshold regions for pion and Δ production.

1. Introduction

Efforts to derive a workable nucleon-nucleon potential from considerations of meson exchange have, in the past, often been based on one-boson exchange models [‡]. This in turn has usually required the introduction of scalar, isoscalar and isovector, σ-mesons, whose role has been to simulate the effects of two-pion exchange, or, in general, to take care of the behavior of the NN potential at intermediate ranges $\approx \frac{1}{2}M_\pi^{-1}$, since clear evidence for the existence of a meson of the desired properties has never been established, this procedure has become less and less satisfying. It is therefore gratifying that, more recently [1–5]), these two-pion exchange effects have

[†] Supported in part by the US National Science Foundation.

[††] Supported in part by the Israel Center for Absorption in Science, the US-Israel Binational Science Foundation and by the US National Science Foundation.

[†††] Present address: Department of Physics, Carnegie-Mellon University, Pittsburgh, Pennsylvania 15213, USA.

[‡] For a recent review of background material on the nucleon-nucleon interaction, see ref. [1]).

yielded to treatment through consideration of box diagrams involving intermediate Δ (1231) isobars (see fig. 1). These diagrams with NΔ or $\Delta\Delta$ intermediate states are then to be included in the NN potential for subsequent iteration between exclusively NN states.

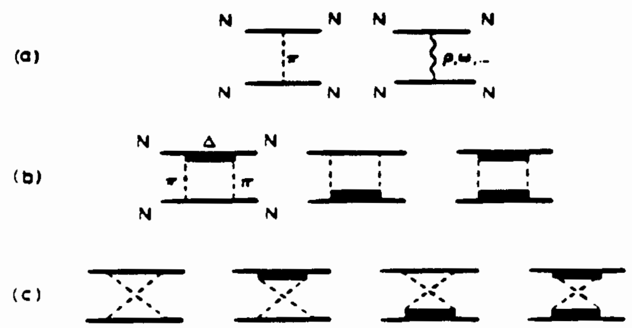

Fig. 1. Ingredients in theories of the NN force. (a) One-pion and other one-meson components of the force. (b) Box diagrams with intermediate Δ(1231) isobars (denoted by heavy lines). (c) Pion crossing in diagrams with intermediate isobars and nucleons.

The calculation of the box diagrams of fig. 1b has thus far been considered for the case of static and nonstatic pions. The nonstatic t-channel dispersion theory involves large extrapolations of the relevant pseudo-physical $N\bar{N} \to \pi\pi$ amplitudes to physical πN scattering amplitudes †. Furthermore, the effect to be discussed in the present work cannot be readily included in this model. The static treatments [e.g. s-channel dispersion theory of ref. [2])] are more in line with the usual attitudes of potential theory taking the baryons to have mass much larger than any other energy which enters into the problem. In particular, the pion exchanges are presumed to take place between roughly "equal" mass baryons and thus the pions are assigned zero energy in the exchange. These pions are consequently far off their mass shell, leading to the characteristic Yukawa estimate that the contribution of a particular exchange diagram comes predominantly at a range given by the reciprocal of the transferred mass in the diagram. Furthermore, because the various intermediate energies are taken equal, the resulting NN potentials have no time dependence, suiting them for ready use in conventional, nonrelativistic potential theory.

The present work is based on the consideration of dynamic effects for the exchanged meson, which, since the Δ-mass permits the isobar to break up into a nucleon and pion, $M_\Delta - M_N > M_\pi$, can in fact take place with the pion on its mass shell and therefore with unrestricted range. Thus, as in the graphs of fig. 2a, the pion can shuttle back and forth repeatedly between the two baryons, mediated by an isobar formation and decay. This modifies the analysis of the NN potential at the range

† For a recent review, see ref. [6]).

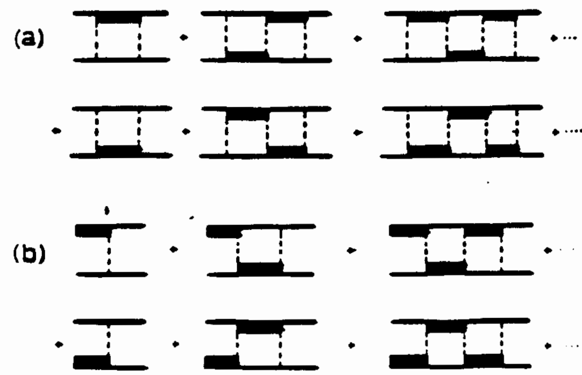

Fig. 2. The primary mechanism under consideration here for (a) NN → NN and (b) NN → NΔ processes. The fact that the isobar-nucleon mass difference is greater than the pion mass, $M_\Delta - M_N > M_\pi$, means that the pion can propagate on-shell, thus making its repeated exchange possible already at the level of ranges ≈ $\frac{1}{2}M_\pi^{-1}$.

$\frac{1}{2}M_\pi^{-1}$, since two of the pions, the first and the last, must in any event be transferred essentially statically in going from and to the initial and final NN configuration. Clearly, the same mechanism can occur for NN → NΔ reactions [and, for that matter, in NΔ → ΔN processes [7,8]), which we do not study here], as shown in fig. 2b. In fact, one may generate the relevant sequence of graphs for both NN → NN and NN → ΔN from the coupled integral equations for the latter process, as shown diagrammatically in fig. 3.

At the present stage, we wish to explore the consequences of this phenomenon in a model case in order to allow for its eventual inclusion in a more complete analysis of the NN force. We shall therefore take spinless and isospinless particles, but with masses M_π, M_N, M_Δ appropriate to the physical situation. We ignore graphs, such as those of fig. 1c, in which two pions are simultaneously present: their contributions

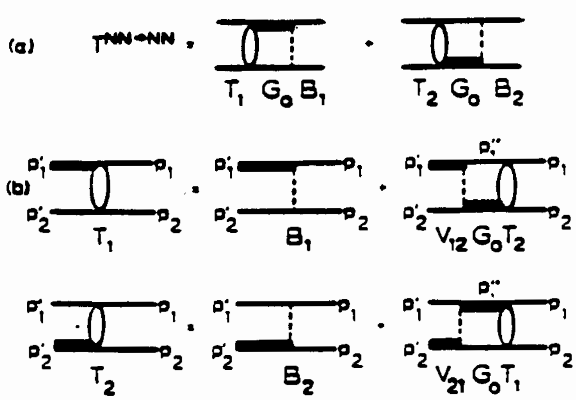

Fig. 3. Integral equations for (a) NN → NN and (b) NN → NΔ reactions extracted from the diagrams of fig. 2, and written formally in eqs. (21) and (13).

have been shown [5]) to involve significant cancellations at momentum transfer $q \approx 3$–$5\ \mathrm{fm}^{-1}$, and we neglect diagonal NΔ and $\Delta\Delta$ interactions whose coupling constants are poorly known. We further do not discuss the exchange of mesons other than the pion, nor do we give a complete analysis of the NN and NΔ coupled channels – restricting ourselves instead to the recurring NΔ configuration of fig. 2, for which the nonstatic multiple pion exchange effects should be maximal. Precisely because of the singularities which arise when the exchanged pions are on shell, and because of the expectation of slow convergence for the successive orders of the diagrams in fig. 2 which is inherent in our mechanism, it is important to start by testing it in as simple a situation as possible. Our restriction to scalar particles precludes a comparison with the dispersion theoretic results mentioned in the foregoing or experimental data on NN → NΔ and NN scattering processes. Subsequently, we hope to study the more realistic problem with nucleon spin and isospin degrees of freedom, full meson exchange, and coupled channels.

In dealing with the integral equations implied by fig. 3, we are immediately faced with a central technical problem, namely whether to handle them as fully relativistic Bethe-Salpeter equations [see, for example, ref. [9])] or to reduce them to covariant equations with, however, three-momentum variables in the manner of Blankenbecler and Sugar [10]). We have chosen the latter route since, after partial wave analysis, the resulting integral equations involve one variable instead of two, which vastly simplifies our analysis. Such an approach is designed to yield a propagator guaranteeing unitarity for the two- and three-particle sectors of the problem under appropriate conditions. However, this constraint is naturally insufficient to determine the full structure of the equations, which would require more dynamical input. Within the approach of Blankenbecler and Sugar [see also refs. [11,12])], after determining the on-shell form of the propagator one still has freedom in choosing its off-shell behavior. Two well-known options are to allow intermediate particles to go off the mass shell symmetrically [10]) or nonsymmetrically [13,14]). Alternatively, one may formulate the entire problem in terms of a quasiparticle approach [15]), in which *inter alia* one characterizes the NΔ propagation in terms of the energy variable and propagator of the isobar subsystem. As we shall see, these various prescriptions lead, in some instances, to rather different numerical results. For the present problem, considerations based on symmetries or on dynamics can, as we shall see, help to motivate a preference amongst these various options.

2. Dynamic equations inferred from two-particle unitarity

The coupled integral equations which sum the diagrams we wish to consider for the NN → NΔ amplitudes can be easily constructed by referring to fig. 3b. Using the total and relative momentum variables

$$P = p_1 + p_2 = p_1' + p_2', \qquad q = \tfrac{1}{2}(p_1 - p_2), \qquad s = P^2, \tag{1}$$

the relevant Bethe-Salpeter equations are

$$\begin{aligned}\langle q'|T_1(s)|q\rangle &= \langle q'|B_1(s)|q\rangle + \int \langle q'|V_{12}(s)|q''\rangle G_0(q'';s)\langle q''|T_2(s)|q\rangle d^4q''/(2\pi)^4,\\ \langle q'|T_2(s)|q\rangle &= \langle q'|B_2(s)|q\rangle + \int \langle q'|V_{21}(s)|q''\rangle G_0(q'';s)\langle q''|T_1(s)|q\rangle d^4q''/(2\pi)^4,\end{aligned} \tag{2}$$

with

$$\langle p'_1p'_2|B_i(s)|p_1p_2\rangle = \frac{gg'}{(p_j-p'_j)^2-M_\pi^2+i\varepsilon}, \qquad \varepsilon\to 0^+, \tag{3}$$

$$\langle p'_1p'_2|V_{ij}(s)|p_1p_2\rangle = \frac{g'^2}{(p_1-p'_1)^2-M_\pi^2+i\varepsilon}, \tag{4}$$

where g and g' are the πNN and πNΔ coupling constants, respectively. Using the conventions of Bjorken and Drell [9]), we shall consider these equations in the two-particle c.m. system, for which

$$\begin{aligned} P &= (\sqrt{s};0), & q &= (0;q),\\ p_1 &= (E_1;q), & p_2 &= (E_2;-q),\\ p'_1 &= (E'_1;q'), & p'_2 &= (E'_2;-q'). \end{aligned} \tag{5}$$

The propagator G_0 appearing in eq. (2) is now to be determined from unitary as suggested by Blankenbecler and Sugar.

A comparison of the unitarity relation

$$T(s^+)-T(s^-) = -iT(s^+)[(2\pi)^4\delta(P_f-\sum_{i=1}^{n}p_i)]T(s^-), \tag{6}$$

where $S_{fi} = \delta_{fi}-i(2\pi)^4\delta(P_f-P_i)T_{fi}$, with the parallel result

$$T(s^+)-T(s^-) = T(s^+)[G_0(s^+)-G_0(s^-)]T(s^-), \tag{7}$$

from eq. (2) yields for the discontinuity $G_0(s^+)-G_0(s^-)$

$$\text{disc}\, G_0(p''_1p''_2;s) = -i(2\pi)^2\delta^+(p''^2_1-m_1^2)\delta^+(p''^2_2-m_2^2). \tag{8}$$

Writing a dispersion relation for the propagator, with the minimal retention of this physical cut only, we have

$$G_0(p''_1p''_2;s) = -2\pi\int\frac{\delta^+(p''^2_1-m_1^2)\delta^+(p''^2_2-m_2^2)}{s'-s-i\eta}ds'. \tag{9}$$

so that

$$G_0(q;s) = -\pi\frac{E''_1+E''_2}{E''_1E''_2}\delta(q_0-\tfrac{1}{2}(E''_1-E''_2))\frac{1}{(E''_1+E''_2)^2-s-i\eta}. \tag{10}$$

We note a point which will be of central importance in the following, namely that other than in eq. (10) the energies E_1'' and E_2'' of the two intermediate particles have here only been fixed for the on-mass-shell situation. Thus we are left with an ambiguity as to how to determine them in V when the propagator is re-inserted into eq. (2). In the following we shall always choose the nucleon intermediate energy in V_{ij} and the phase space factor to be fixed by its on-shell value

$$E_N(q) = (M_N^2+q^2)^{\frac{1}{2}}, \tag{11}$$

whereas the isobar energy is determined by one of two prescriptions: (i) the "symmetric" situation in which the isobar is also put on shell

$$E_\Delta(q) = (s_\Delta+q^2)^{\frac{1}{2}}, \qquad s_\Delta = M_\Delta^2, \tag{12a}$$

and (ii) the "nonsymmetric" case where the isobar energy is fixed from energy conservation at the intermediate stage,

$$E_\Delta(q) = (s_\Delta+q^2)^{\frac{1}{2}}, \qquad s_\Delta = s-2\sqrt{s}E_N+M_N^2. \tag{12b}$$

It is important to note that the nonsymmetric prescription has two advantages over the symmetric one, and is therefore much to be preferred. Firstly, by denying sufficient energy for Δ-production in the intermediate state in the subthreshold situation, it prevents an artificial appearance of pion on-shell propagation there. Hence the threshold singularity in V_{ij} is not reached in the integral equation, while the on-shell choice, eq. (12a) always purports to allow for a true intermediate isobar. Secondly, by providing intermediate, off-shell phase space appropriate to the energy of the "isobar" produced above threshold, the nonsymmetric choice yields suitably time-reversal invariant amplitudes. This is expressed, for instance, in the symmetry of the resulting NN → NN amplitude, which is not present for the prescription of eq. (12a). This consideration is borne out by our numerical results. Despite the clear preference for the nonsymmetric choice, in which only the nucleon is placed on the mass shell, we shall below show results for both cases for the sake of comparison and in view of the fact that this ambiguity is well known to be intrinsic to the approaches related to that of Blankenbecler and Sugar [10-14]).

We now rewrite eq. (2) in an explicit form, taking advantage of the symmetry in B_f and V_{ij} which is present for the spinless case and which permits us to decouple the integral equations trivially. We obtain

$$\langle q'|T(s)|q\rangle = \frac{gg'}{2M_N^2-M_\pi^2-2E_NE_N'+2q\cdot q'} - \int\frac{g'^2}{M_N^2+s_\Delta-M_\pi^2-2E_\Delta'E_N''+2q'\cdot q''+i\varepsilon}$$
$$\times\frac{E_N''+E_\Delta''}{2E_N''E_\Delta''}\,\frac{1}{(E_N''+E_\Delta'')^2-s-i\eta}\langle q''|T(s)|q\rangle\frac{d^3q''}{(2\pi)^3}, \tag{13}$$

for $T_1 = T_2 = T$. Partial-wave analysis for B, V and T in the form

$$\langle q'|T(s)|q\rangle = \sum_{L=0}^{\infty}\langle q'|T_L(s)|q\rangle P_L(\hat{q}'\cdot\hat{q}), \tag{14}$$

then yields

$$\langle q'|T_L(s)|q\rangle = \langle q'|B_L|q\rangle - \frac{4\pi}{2L+1}\int_0^\infty \langle q'|V_L(s)|q''\rangle \times \frac{E''_N+E''_\Delta}{2E''_N E''_\Delta}\frac{1}{[E''_N+E''_\Delta]^2-s-i\eta}\langle q''|T_L(s)|q\rangle \frac{q''^2 dq''}{(2\pi)^3}, \quad (15)$$

where

$$\langle q'|B_L|q\rangle = -\frac{gg'}{2qq'}(2L+1)Q_L\left(\frac{2E_N E'_N + M_\pi^2 - 2M_N^2}{2qq'}\right), \quad (16)$$

$$\langle q'|V_L(s)|q\rangle = -\frac{g'^2}{2qq'}(2L+1)Q_L\left(\frac{2E_N E'_\Delta + M_\pi^2 - M_N^2 - s_\Delta - i\varepsilon}{2qq'}\right), \quad (17)$$

in terms of Legendre functions of the second kind. It is easily seen from eq. (13) or (17) that the singularities in V, indicating pion propagation on the mass shell, are encountered under the approriate kinematical circumstances (while, of course, in B they are not). This is a characteristic of the present approach, which is therefore quite distinct from static approximations. Mercifully, from the point of view of numerical work, the partial wave analysis tones down the impact of these singularities quite considerably, since they are then only logarithmic in character.

Despite the basically two-particle nature of the present approach, we must still be concerned with the possibility of a three-particle intermediate contribution, at least to the extent that it endows the isobar – and therefore our nucleon-isobar propagator – with a width. This we introduce in a semiphenomenological way by

Fig. 4. (a) The self-energy of the Δ-isobar and (b) its decay vertex, as used to incorporate the isobar width into its propagator and hence into the NΔ propagator G_0.

calculating the self-energy of the Δ-propagator (or equivalently the Δ-decay width, see fig. 4), which in the usual way [9] undergoes the replacement

$$\frac{1}{p^2-M_\Delta^2} \to \frac{1}{p^2-s_\Delta-i\sqrt{s_\Delta}\Gamma}, \quad (18)$$

with

$$\Gamma(s_\Delta) = \frac{kg'^2}{8\pi s_\Delta}, \qquad (M_N^2+k^2)^{\frac{1}{2}}+(M_\pi^2+k^2)^{\frac{1}{2}} = \sqrt{s_\Delta}. \quad (19)$$

This in turn is introduced into G_0, the two-particle propagator, by taking

$$\eta = \begin{cases} (M_N + \sqrt{s_\Delta})\Gamma, & \sqrt{s_\Delta} > M_N + M_\pi \\ \varepsilon, & \sqrt{s_\Delta} \leqq M_N + M_\pi \end{cases} \tag{20}$$

in eq. (15). These somewhat *ad hoc* procedures are improved upon in the quasiparticle formalism discussed in the next section, which, however, is not a panacea for all the ills of the problem, as we shall see. Lastly, we note that the amplitude for the NN → NN precesss is easily obtained from that for NN → NΔ of eqs. (13) and (15) through

$$\langle \boldsymbol{q}'|T^{NN-NN}(s)|\boldsymbol{q}\rangle = -\int \langle \boldsymbol{q}'|B|\boldsymbol{q}''\rangle \frac{E''_N + E''_\Delta}{2E''_N E''_\Delta} \frac{1}{(E''_N + E''_\Delta)^2 - s - i\eta} \times \langle \boldsymbol{q}''|T^{NN-N\Delta}(s)|\boldsymbol{q}\rangle \mathrm{d}^3 q''/(2\pi)^3. \tag{21}$$

Before turning to the calculational results based on the method of this section, we shall first examine the quasiparticle model for producing a unitary, three-dimensional integral equation, in an attempt to treat the three-particle sector and isobar decay width more properly.

3. Dynamic equations using two- and three-particle unitarity

The quasiparticle approach [15]) takes as its point of departure unitarity in both two- and three-particle sectors and uses these to determine the dynamical elements of the integral equations, which will here be taken in a coupled-channel form. The channels in question will be those of the NN and NΔ two-baryon states. In both cases the second baryon will be viewed as a πN composite, that is, the second nucleon of the NN channel is a bound πN state having the mass of the nucleon, and the

Fig. 5. Diagrammatic representation of coupled integral equations in the quasiparticle approach. The dotted line represents the quasiparticle, a (πN) composite which may be either bound, to produce the nucleon, or resonating, to produce the isobar.

Δ-isobar is, of course, a πN resonance. For reactions involving two particles, we have (see fig. 5)

$$\langle p'; \beta|T(s)|p; \alpha\rangle = \langle p'; \beta|B(s)|p; \alpha\rangle + \sum_\gamma \int \langle p'; \beta|B(s)|p''; \gamma\rangle \times \mathcal{G}_\gamma(p''; s)\langle p''; \gamma|T(s)|p; \alpha\rangle \mathrm{d}^4 p''/(2\pi)^4, \quad \{\alpha, \beta, \gamma\} = \{NN, N\Delta\}. \tag{22}$$

The kinematic variables are particle momenta in the two- and three-particle c.m. systems and unitarity conventions are as before. Since we now allow for contributions to unitarity from the three-particle sector, we must broaden our considerations concerning discontinuities according to [12,15])

$$T(s^+)-T(s^-) = T(s^+)[\mathcal{G}(s^+)-\mathcal{G}(s^-)]\,T(s^-)+T(s^+)\mathcal{G}(s^+)[B(s^+)-B(s^-)]\mathcal{G}(s^-)T(s^-), \tag{23}$$

leading to

$$\begin{aligned}
&\langle p_1'p_2'|T(s^+)|p_1p_2\rangle-\langle p_1'p_2'|T(s^-)|p_1p_2\rangle \\
&\quad = -i\int(2\pi)^4\delta(P-p_1''-p_2'')\langle p_1'p_2'|T(s^+)|p_1''p_2''\rangle(2\pi)^2\delta^+(p_1''^2-m_1^2)\delta^+(p_2''^2-m_2^2) \\
&\quad\times\langle p_1''p_2''|T(s^-)|p_1p_2\rangle \mathrm{d}^4p_1''\mathrm{d}^4p_2''/(2\pi)^8 \\
&\quad -i\int(2\pi)^4\delta(P-p_1''-p_2''-p_3'')\langle p_1p_2|T(s^-)|p_1''p_2''p_3''\rangle \\
&\quad\times(2\pi)^3\delta^+(p_1''^2-m_1^2)\delta^+(p_2''^2-m_2^2)\delta^+(p_3''^2-m_3^2) \\
&\quad\times\langle p_1''p_2''p_3''|T(s^-)|p_1p_2\rangle \mathrm{d}^4p_1''\mathrm{d}^4p_2''\mathrm{d}^4p_3''/(2\pi)^{12}.
\end{aligned} \tag{24}$$

The three-particle break-up amplitude which has been introduced here is given by

$$\langle p_1'p_2'|T(s)|p_1p_2p_3\rangle = \sqrt{\tfrac{1}{3}}\sum_n\langle p_1'p_2'|T(s)|p_1(n)p_2(n)\rangle g(\sigma_n)v_n, \tag{25}$$

where the summation is over the two-baryon subsystems, g is the propagator for that subsystem shortly to be determined, and v_n is the relevant quasiparticle dissociation vertex.

We now introduce the spectator assumption for the two-particle propagator, assuming, in our case, that the (noncomposite) nucleon is always on its mass shell,

$$\mathcal{G}(p) = 2\pi\delta^+(p^2-M_N^2)g(\sigma_p), \qquad \sigma_p \equiv (P-p)^2. \tag{26}$$

Designating for first consideration the case in which the pion in the unitarity relation is transferred between two different nucleons (fig. 6a), we can compare eqs. (23)

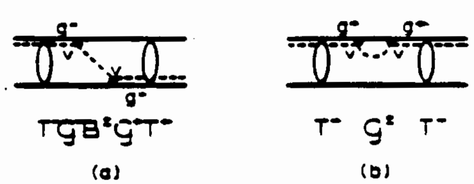

Fig. 6. Two contributors to the right-hand side of the unitarity relation of eq. (23), one (a) involving exchange of a pion and determining the interaction B, the other (b) involving transfer on the same baryon and determining the quasiparticle propagator g.

and (24) to yield for the interaction

$$\langle p'|B(s^+)|p\rangle - \langle p'|B(s^-)|p\rangle = -iv2\pi\delta^+((P-p-p')^2 - M_\pi^2)v. \tag{27}$$

It is then easy to show that

$$(P-p-p')^2 - M_\pi^2 = (\sqrt{s}-W)(\sqrt{s}-W+2\omega_{p+p'}), \tag{28}$$

where

$$W = E_N + E'_N + \omega_{p+p'} = \sqrt{p^2+M_N^2} + \sqrt{p'^2+M_N^2} + \sqrt{(p+p')^2+M_\pi^2}. \tag{29}$$

It is consistent with the restriction to three-particle states in this model that we ignore [15]) the zero arising from the backward-going pion in the second factor of eq. (28) to write

$$\delta((P-p-p')^2 - M_\pi^2) \approx \frac{W}{\omega_{p+p'}}\delta(s-W^2). \tag{30}$$

Hence the dispersion relation with minimal singularity structure yields for the interaction

$$\langle p'|B(s)|p\rangle = \frac{1}{2\pi i}\int \frac{\mathrm{disc}\,\langle p'|B(s')|p\rangle}{s'-s-i\varepsilon}\,\mathrm{d}s' = -v\frac{W}{\omega_{p+p'}(W^2-s-i\varepsilon)}v. \tag{31}$$

It should be noted that, above production threshold, the singularity arising from the vanishing of the denominator in the interaction of eq. (31) can be encountered in the fully off-shell situation even for the driving term in eq. (22). Although this does not appear to cause any basic difficulty in the theory, it does lead to much larger Born terms for the NN → NΔ amplitude than those of the method discussed in the previous section, which are related directly to Feynman diagrams. We have therefore treated the result of the quasiparticle approach with some wariness.

For the case of the pion transferred on the same baryon line (fig. 6b), the spectator assumption immediately leads to the result for the quasiparticle propagator

$$g(\sigma_p^+) - g(\sigma_p^-) = -2\pi i\delta^+(\sigma_p - M_b^2) - ig(\sigma_p^+)g(\sigma_p^-)$$
$$\times \int v\frac{E_{p'}+\omega_{p'}}{2E_{p'}\omega_{p'}}\delta(p''_0)\delta(\sigma_p-(E_{p'}+\omega_{p'})^2)v\frac{\mathrm{d}^4p''}{(2\pi)^4}, \qquad b = \mathrm{N}, \Delta, \tag{32}$$

which can be solved approximately using the N/D method to give

$$g(\sigma_p) \approx \left[\sigma_p - M_b^2 + \int\frac{E_{p'}+\omega_{p'}}{2E_{p'}\omega_{p''}}\frac{vv}{(E_{p'}+\omega_{p'})^2-\sigma_p-i\varepsilon}\frac{\mathrm{d}^3p''}{(2\pi)^3}\right]^{-1}. \tag{33}$$

We now combine eqs. (22), (26), (31) and (33) and restrict our consideration to intermediate NΔ channels only, in order to focus once again on the case of the diagrams of fig. 2. Again exploiting the symmetry of the spinless case, we arrive at †

† Eq. (34) allows us to identify the present coupling constants with those of the previous section when we compare the corresponding integral equations in the static limit.

$$\langle q'|T(s)|q\rangle = \frac{-2gg'(E_N+E'_N+\omega_{q+q'})}{\omega_{q+q'}[(E_N+E'_N+\omega_{q+q'})^2-s-i\varepsilon]}$$
$$-\int \frac{2g'^2(E'_N+E''_N+\omega_{q'+q''})}{\omega_{q'+q''}[(E'_N+E''_N+\omega_{q'+q''})^2-s-i\varepsilon]} \frac{1}{2E''_N} g(\sigma'_q)\langle q''|T(s)|q\rangle \frac{d^3q''}{(2\pi)^3}, \tag{34}$$

for the NN $\rightarrow$ NΔ amplitude, and

$$\langle q'|T^{NN\rightarrow NN}(s)|q\rangle = -\int \frac{gg'(E'_N+E''_N+\omega_{q'+q''})}{\omega_{q'+q''}[(E'_N+E''_N+\omega_{q'+q''})^2-s-i\varepsilon]}$$
$$\times \frac{1}{E''_N} g(\sigma_{q''})\langle q''|T(s)|q\rangle \frac{d^3q''}{(2\pi)^3}, \tag{35}$$

for the NN $\rightarrow$ NN amplitude. The partial wave analysis of these equations proceeds as in eqs. (14) and (15) and can be carried out analytically although it does not lead directly to simple, well-known forms as in eqs. (16) and (17). In dealing with the isobar propagator $g(\sigma_q)$ (the nucleon case no longer enters for the diagrams of fig. 2), we note that the imaginary part of the integral in eq. (33) is simply the isobar width of eq. (19). We take the real part to be approximated by a constant which renormalizes the isobar mass to its observed value,

$$g(\sigma_q) \approx [\sigma_q - M_\Delta^2 + i\sqrt{\sigma_q}\Gamma(\sigma_q)]^{-1}. \tag{36}$$

Eqs. (34) and (35) in the quasiparticle method are to be compared with eqs. (13) and (21) of the previous section. In the static limit ($M_N \approx M_\Delta \gg M_\pi$) they are identical. Away from this limit they are distinguished by the fact that the quasiparticle method elects to introduce a specific form of the clustering property [9-12,15]) directly into the dynamic equations, so that only the isobar invariant energy appears in the propagator, whereas in eqs. (13) and (21) the total (nucleon plus isobar) energy enters. The essential computational difference between the two approaches comes, however, from the off-energy-shell singularity in the driving term of eq. (34), as we have noted above. This feature † tends to lead to much larger values for this term than are inferred from the corresponding one-pion-exchange Feynman graph, the two results approaching each other only very near the static limit. In fact, in the off-shell limiting situation $q, q' \rightarrow 0$, while $s = 4(M_N+T_N^{c.m.})^2$, one easily sees from eqs. (13) and (34) that the ratio of the driving terms of sects. 2 and 3 is approximately

$$(1-2T_N^{c.m.}/M_\pi)^{-1}, \tag{37}$$

so that even at quite low energies, say $T_N^{c.m.} = 50$ MeV, the quasiparticle method gives a much larger result.

† This consideration should also enter to some degree for applications of the quasiparticle method to πd scattering [16]), though it presumably would be less relevant in the case of the original use for πN scattering [15]).

4. Results

In carrying out the present calculation, we choose particle masses to parallel the physical situation for the $\pi N\Delta$ system, $M_\pi = 140$ MeV, $M_N = 939$ MeV, $M_\Delta = 1231$ MeV. Correspondingly, the coupling constants are taken as $g = 13.5\ M_\pi$, as implied by the usual πNN pseudoscalar value, $g^2_{\pi NN}/4\pi = 14.6$, and $g' = 3.47\ M_\Delta$, from eq. (19) with $\Gamma(M_\Delta^2) = 111$ MeV.

Numerical solution of the integral equations could proceed by contour rotation and matrix inversion or by the method of Padé approximants [17]. We elected the latter method which proved both straightforward and reliable. The diagonal approximant was used, and six iterations of the series sufficed for solutions accurate to $1:10^4$ or $1:10^5$, as checked each time by reinserting into the right-hand side of the integral equation and comparing. A graphic way to see the consequences of our mechanism was to go to the static limit,

$$2E_N E'_N - 2M_N^2 \to q^2 + q'^2, \qquad 2E_N E'_\Delta - M_N^2 - s_\Delta \to q^2 + q'^2, \tag{38}$$

in eqs. (16) and (17) for instance, and observe the more rapid convergence of the Padé procedure.

We found that either Simpson or Gaussian integration was adequate, with about 80 to 100 points required and an upper limit of the infinite integration range taken at 8 fm^{-1}, after which further increase by 30 % or so in either parameter led to no significant changes in numerical accuracy. Since the integration carries the interaction term V through the pion on-mass-shell singularity, the choice of the "infinitesimal" ε was of some consequence. Once a sufficiently small value was used, further reduction by one and two orders of magnitude produced numerical changes of at most a few percent, and generally less than 1 %.

The largest effects of the nonstatic mechanism were seen in the $L = 0$ partial wave, and we therefore concentrate on it. For $L = 1$, the amplitudes were adequately represented, to within about 10 % to 15 %, by their Born terms plus box diagrams at the energies considered here (c.m. kinetic energy $T_N^{\text{c.m.}} \leq 175$ MeV). Well below threshold, at $T_N^{\text{c.m.}} = 50$ MeV, the highly off-shell NN $\to N\Delta$ amplitudes given by the approach of sect. 2 with the symmetric or nonsymmetric prescriptions [eqs. (12a) or (12b)] are very similar, as seen in fig. 7a. We have already noted that the nonsymmetric procedure is to be preferred for its observance of time-reversal invariance in this problem, a property valid to $1:10^8$ at $T_N^{\text{c.m.}} = 50$ MeV and $1:10^4$ at $T_N^{\text{c.m.}} = 175$ MeV in that case, but violated by 50 % or more in certain instances at 175 MeV when the symmetric prescription is used. In all results based on the method of sect. 2 at $T_N^{\text{c.m.}} = 50$ MeV, the amplitudes are adequately approximated by box diagrams for the off-energy-shell NN $\to$ NΔ case. This is much less true for the resulting NN $\to$ NN amplitudes, even at $T_N^{\text{c.m.}} = 50$ MeV, shown in fig. 7b. The NN $\to$ NΔ results at 175 MeV, see fig. 8, have much larger qualitative deviations between the symmetric, nonsymmetric and static prescriptions of eqs. (12) and (38) than do the

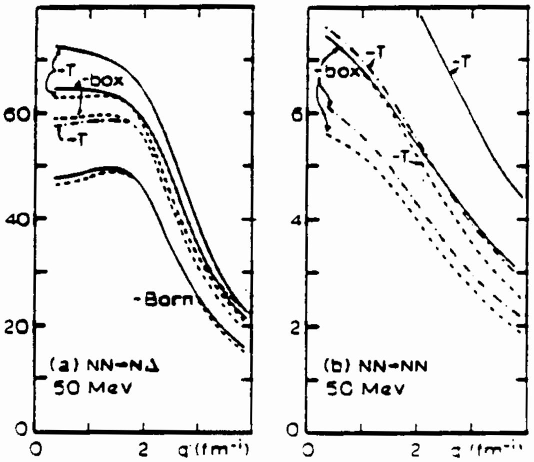

Fig. 7. Fully off-energy-shell amplitudes of eqs. (15) and (21) for the (a) NN → NΔ and (b) NN → NN reactions below production threshold at $T_N^{c.m.} = 50$ MeV and for the $L = 0$ partial wave. All results are for $q = 2$ fm^{-1}. "Born" refers to the first diagram of fig. 2b and "box" to its sum with the second for NN → NΔ, or to the first graph of fig. 2a for NN → NN. The full summation of the graphs in fig. 2 yields the amplitude labeled T. Solid lines refer to the nonsymmetric prescription of eq. (12b), dashed lines to the static case, eq. (38), and dot-dash lines to the symmetric choice, eq. (12a).

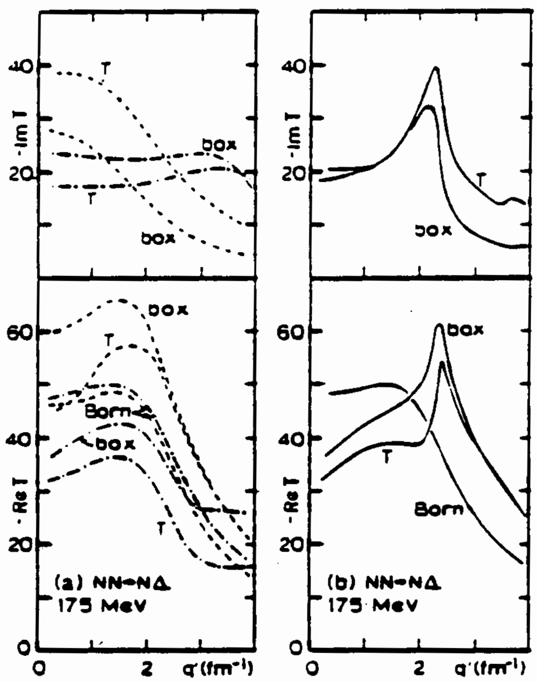

Fig. 8. Fully off-energy-shell NN → NΔ amplitudes above production threshold for $T_N^{c.m.} = 175$ MeV. Other definitions and conventions as in fig. 7.

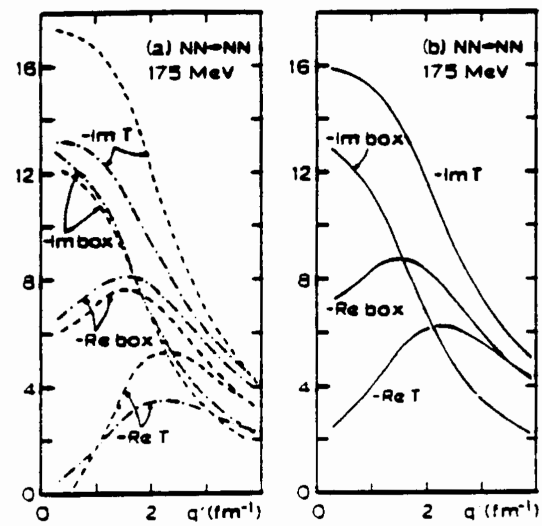

Fig. 9. Fully off-energy-shell NN → NN amplitudes above production threshold for $T_N^{c.m.}$ = 175 MeV. Other definitions and conventions as for fig. 7.

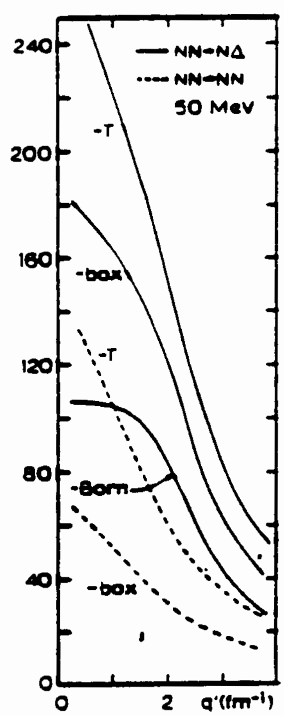

Fig. 10. Fully off-energy-shell amplitudes below production threshold for $T_N^{c.m.}$ = 50 MeV in the quasiparticle approach [15]) discussed in sect. 3. Other definitions and conventions as for fig. 7, except that here solid lines refer to NN → NΔ and dashed lines to NN → NN.

below-threshold amplitudes. This is, of course, as one would have expected for the dynamic mechanism considered here. However, for nucleon-nucleon scattering, fig. 9, the differences are greatly muted by the further integration over the propagator and Born term, though they still amount to quantitative effects of 10 % or 20 %. We note that the nonsymmetric prescription for intermediate off-mass-shell behavior, which we believe to be the greatly preferred approach for the physical reasons of time-reversal invariance and the onset of isobar effects sketched below eq. (12), generally differs quite substantially from the results of the conventional static approach.

Lastly, we turn to the amplitudes in fig. 10, given by the quasiparticle method of sect. 3. These are shown only for the 50 MeV case, since the off-energy-shell singularity in the driving term of that method, discussed in connection with eq. (37), makes the approach highly suspect for the present application when used above production threshold. Even at 50 MeV, this same consideration leads to very different results from those obtained previously. This arises essentially from the factor of eq. (37) in the $NN \rightarrow N\Delta$ driving term, and its square in $NN \rightarrow NN$ elastic scattering.

We conclude that nonstatic effects for multiple pion exchange with repeated production and decay of intermediate isobars yield significant quantitative, and occasionally qualitative, differences from the conventional approximation of Born terms (for $NN \rightarrow N\Delta$) or static box diagrams. They should therefore be included in more complete calculations which take into account spin and isospin, the exchange of heavier mesons, and complete coupling between NN and $N\Delta$ channels.

One of us (J.M.E.) wishes to acknowledge with thanks the kind hospitality of the University of Virginia, where the major portion of this work was carried out, and useful discussions with W. Kloet and R. Silbar. We are also grateful for the assistance of the Computer Science Center of the University of Virginia.

References

1) G. E. Brown and A. D. Jackson, The nucleon-nucleon interaction (North-Holland, Amsterdam, 1976); K. Erkelenz, Phys. Reports 13C (1974) 191
2) H. Sugawara and F. von Hippel, Phys. Rev. 172 (1968) 1764; 185 (1969) 2046
3) S. Jena and L. S. Kisslinger, Ann. of Phys. 85 (1974) 251
4) A. M. Green and P. Haapakoski, Nucl. Phys. A221 (1974) 429
5) R. A. Smith and V. R. Pandharipande, Nucl. Phys. A256 (1976) 327
6) R. Vinh Mau, Proc. Int. Top. Conf. on meson-nuclear physics, ed. P. Barnes *et al.* (AIP, 1976), p. 642
7) V. A. Karmanov, L. A. Kondratyuk and I. S. Shapiro, JETP (Sov. Phys.) 34 (1972) 1172 [ZhETF (USSR) 61 (1971) 2185]
8) H. Arenhövel, Nucl. Phys. A247 (1975) 473
9) J. D. Bjorken and S. D. Drell, Relativistic quantum fields (McGraw-Hill, New York, 1965)
10) R. Blankenbecler and R. Sugar, Phys. Rev. 142 (1966) 1051
11) V. A. Alessandrini and R. L. Omnes, Phys. Rev. 139 (1965) B167
12) D. Z. Freedman, C. Lovelace and J. M. Namyslowski, Nuovo Cim. 43A (1966) 258
13) F. Gross, Phys. Rev. 186 (1969) 1448
14) K. Erkelenz and K. Holinde, Z. Naturf. 28a (1973) 353
15) R. Aaron, R. D. Amado and J. E. Young, Phys. Rev. 174 (1968) 2022
16) R. M. Woloshyn, E. J. Moniz and R. Aaron, Phys. Rev. C13 (1976) 286
17) G. A. Baker, Jr. and J. L. Gammel, ed., The Padé approximant in theoretical physics (Academic Press, New York, 1970)